

## TITLE PAGE

# DEVELOPING NEW DUAL-ACTION ANTIVIRAL/ANTI-INFLAMMATORY SMALL MOLECULES FOR COVID-19 TREATMENT USING IN SILICO AND IN-VITRO APPROACHES

**Short Title:** ANTIVIRAL AND ANTI-INFLAMMATORY SMALL MOLECULES FOR COVID-19 TREATMENT

Vladimir V. Ivanov <sup>1</sup>†, Anton B. Zakharov <sup>1</sup>, Dmytro O. Anokhin <sup>1</sup>, Olha O. Mykhailenko <sup>2</sup>, Sergiy M. Kovalenko <sup>1</sup>, Larysa V. Yevsieieva <sup>1</sup>, Victoriya A. Georgiyants <sup>2\*</sup>, Michal Korinek <sup>3,4</sup>†, Yu-Li Chen <sup>5</sup>, Shu-Yen Fang <sup>4,6</sup>, Mohamed El-Shazly<sup>7</sup>, Tsong-Long Hwang <sup>4,5,8\*</sup>, Oleg M. Kalugin <sup>1</sup>

<sup>1</sup> School of Chemistry, V. N. Karazin Kharkiv National University, Kharkiv 61077, Ukraine.

[vivanov@karazin.ua](mailto:vivanov@karazin.ua), <https://orcid.org/0000-0003-2297-9048> (V.V.I.); [abzakharov@karazin.ua](mailto:abzakharov@karazin.ua),

<https://orcid.org/0000-0002-9120-8469> (A.B.Z.); [dmitriy25102002@gmail.com](mailto:dmitriy25102002@gmail.com),

<https://orcid.org/0000-0002-4958-2692> (D.O.A.);

[sergiy.m.kovalenko@karazin.ua](mailto:sergiy.m.kovalenko@karazin.ua), <https://orcid.org/0000-0003-2222-8180> (S.M.K.);

[lar0858@gmail.com](mailto:lar0858@gmail.com), <https://orcid.org/0000-0002-8427-7036> (L.V.Y); [onkalugin@gmail.com](mailto:onkalugin@gmail.com),

<https://orcid.org/0000-0003-3273-9259> (O.M.K.)

<sup>2</sup> Department of Pharmaceutical Chemistry, National University of Pharmacy, Kharkiv 61002,

Ukraine. [o.mykhailenko@nuph.edu.ua](mailto:o.mykhailenko@nuph.edu.ua); <https://orcid.org/0000-0003-3822-8409> (O.O.M.);

[vgeor@nuph.edu.ua](mailto:vgeor@nuph.edu.ua); <https://orcid.org/0000-0001-8794-8010> (V.A.G.)

<sup>3</sup> Graduate Institute of Natural Products, College of Pharmacy, Kaohsiung Medical University,

Kaohsiung 80708, Taiwan. [michalk@kmu.edu.tw](mailto:michalk@kmu.edu.tw), <https://orcid.org/0000-0002-8988-8610> (M.K.)

<sup>4</sup> Graduate Institute of Natural Products, College of Medicine, Chang Gung University, Taoyuan

33302, Taiwan. [d1001501@cgu.edu.tw](mailto:d1001501@cgu.edu.tw) (S.-Y.F.),

<sup>5</sup> Graduate Institute of Health Industry Technology and Research Center for Chinese Herbal

Medicine, College of Human Ecology, Chang Gung University of Science and Technology, Taoyuan

33303, Taiwan [oo66931@gmail.com](mailto:oo66931@gmail.com), <https://orcid.org/0000-0003-2392-1702> (Y.-L.C.);

[htl@mail.cgust.edu.tw](mailto:htl@mail.cgust.edu.tw), <https://orcid.org/0000-0002-5780-3977> (T.-L.H.),

<sup>6</sup> Graduate Institute of Biomedical Sciences, College of Medicine, Chang Gung University, Taoyuan

33302, Taiwan.

<sup>7</sup> Department of Pharmacognosy, Faculty of Pharmacy, Ain Shams University, Cairo 11566, Egypt.

[mohamed.elshazly@pharma.asu.edu.eg](mailto:mohamed.elshazly@pharma.asu.edu.eg) <https://orcid.org/0000-0003-0050-8288> (M.E.S.)

<sup>8</sup> Department of Anesthesiology, Chang Gung Memorial Hospital, Taoyuan 33305, Taiwan

\* Corresponding authors: [vgeor@nuph.edu.ua](mailto:vgeor@nuph.edu.ua) (V.A.G.); [htl@mail.cgust.edu.tw](mailto:htl@mail.cgust.edu.tw) (T.-L.H.); Tel.: +380572-67-91-97 (V.G.); +886-3-2118800 (ext. 5523) (T.-L.H.)

NOTE: This preprint reports new research that has not been certified by peer review and should not be used to guide clinical practice.

36  
37 † These authors contributed equally to this work

## 38 39 **Abstract**

40 This study aims to develop new molecular structures as potential therapeutic agents  
41 against COVID-19, utilizing both *in silico* and *in vitro* studies. Potential targets of  
42 cepharanthine (CEP) against COVID-19 to reveal its underlying mechanism of action  
43 were evaluated using *in silico* screening experiments. A library of new molecules was  
44 docked into the receptor binding domain of the SARS-CoV-2 spike glycoprotein  
45 complex with its receptor, human ACE2, to identify promising compounds. Receptor-  
46 oriented docking was performed using the most likely macromolecular targets, aimed  
47 at inhibiting key viral replication pathways and reducing inflammatory processes in  
48 damaged tissues. The hit molecules showed potential inhibition of Mpro and PLpro  
49 proteases of SARS-CoV-2, which are involved in viral replication. They also showed  
50 a potential inhibitory effect on Janus kinase (Jak3), which mediates intracellular  
51 signaling responsible for inflammatory processes.

52 The *in vitro* study examined the effects of the selected hit molecules on the generation  
53 of superoxide anions and the release of elastase in activated neutrophils, which are  
54 factors that exacerbate tissue inflammation and worsen the clinical manifestations of  
55 COVID-19. It was demonstrated that 2-((5-((4-isopropylphenyl)sulfonyl)-6-oxo-1,6-  
56 dihydropyrimidin-2-yl)thio)-N-(3-methoxyphenyl)acetamide (**Hit15**) inhibited virus  
57 infection by 43.0% at 10  $\mu$ M using pseudovirus assay and suppressed fMLF/CB-  
58 induced superoxide anion generation and elastase release in human neutrophils with

59 IC<sub>50</sub> values 1.43 and 1.28  $\mu\text{M}$ , respectively. **Hit15** showed promising activity against  
60 coronavirus that can be further developed into a therapeutic agent.

61 **Keywords:** synthetic compounds, viral entry and replication, spike, SARS-CoV-2,  
62 neutrophils

63

## 64 **Introduction**

65 The recent trends in the search for effective drugs against COVID-19 focus on the  
66 development of inhibitors of key SARS-CoV-2 proteins. Integrating antiviral and anti-  
67 inflammatory therapy is a critical approach to managing COVID-19 since the  
68 inflammation caused by the immune response leads to serious complications of the  
69 disease [1, 2].

70 Understanding the pathological progression and clinical manifestations of COVID-19  
71 is a prerequisite for the development of drugs for rational therapeutic intervention. The  
72 challenge of developing effective drugs to combat SARS-CoV-2 remains unresolved.  
73 There is an urgent need for medications that can suppress the main mechanisms of  
74 SARS-CoV-2 replication within the cell and mitigate the consequences of its impact  
75 on the human body [3]. This need has become especially relevant with the emergence  
76 of new viral variants capable of evading immune protection provided by vaccines [4,  
77 5].

78 COVID-19, caused by the SARS-CoV-2 virus, is a complex, multi-organ, and  
79 heterogeneous disease. The clinical manifestations of COVID-19 are diverse. The  
80 disease can progress from uncomplicated forms to pneumonia and acute respiratory

81 distress syndrome (ARDS), requiring intensive care [6]. The pathogenesis of COVID-  
82 19 is driven by a hyperactive inflammatory response, leading to severe inflammation  
83 and tissue damage, particularly in the lungs [7]. It is known that excessive neutrophil  
84 activation causes tissue damage, and the neutrophil activation pathway plays a key role  
85 in the poor prognosis of COVID-19 patients by exacerbating lung inflammation and  
86 respiratory failure. Activated neutrophils secrete several cytokines, including  
87 superoxide anion, which can directly or indirectly cause tissue damage. Neutrophil  
88 elastase is a major product secreted by activated neutrophils and a key factor in tissue  
89 destruction in inflammatory diseases [8]. The inhibition of superoxide formation and  
90 elastase release, which are the markers of the anti-inflammatory response, can reduce  
91 the inflammatory burden and limit damage to the lungs and other tissues caused by  
92 COVID-19 [9].

93 The integration of antiviral and anti-inflammatory therapies is a key approach to  
94 managing COVID-19. This approach was initially utilized, for example, with the  
95 introduction of corticosteroids into treatment regimens to reduce the body's  
96 inflammatory response [1, 2]. In this context, there is growing interest in biologically  
97 active substances from the plant *Jordanian hawksbeard*, as they possess both anti-  
98 inflammatory and antiviral properties. These substances inhibited the main protease of  
99 SARS-CoV-2 and reduced inflammatory processes [8, 10].

100 Studies confirmed the *in vitro* and *in vivo* antiviral potential of cepharanthine (CEP)  
101 against SARS-CoV-2. CEP demonstrated multiple molecular mechanisms, including  
102 the suppression of the viral entry phase (by interacting with the viral spike protein and

103 blocking its binding to ACE2) and reducing the production of inflammatory factors  
104 [11, 12].

105 Approaches that enable the targeted creation of new pharmacologically active  
106 molecules were implemented in previous studies including computer-aided molecular  
107 modeling (CAMM) and QSAR methods [13]. In our search for new agents against  
108 SARS-CoV-2, we used workflows that combine several tools, such as pharmacophore  
109 screening of large chemical spaces and molecular docking of preselected candidates  
110 [14].

111 In this study, we used *in silico* screening experiments and receptor-oriented docking in  
112 the receptor binding domain of the SARS-CoV-2 Omicron spike glycoprotein complex  
113 with its receptor, human ACE2. We also used the three-dimensional structural models  
114 of other active sites of biological molecules involved in the mechanisms of SARS-  
115 CoV-2's impact on the body, using cepharanthine as a representative structure.

116

## 117 **Materials and Methods**

### 118 **Computational Procedures**

119 Molecular ligand analysis and the design of new biologically active molecules were  
120 performed using free and publicly available software packages including Jmol [15],  
121 PyMol [16], and LigandScout 4.4 [17, 18], which allowed for the pharmacophore  
122 analysis and virtual screening of specific molecular databases relative to the generated  
123 pharmacophore.

124 LigandScout tools [18] were used to identify the molecular parameters that would  
125 correspond to drug-like properties. Molecules with poor permeability and oral  
126 absorption (molecular weight > 500, C logP > 5, more than five hydrogen bond donors,  
127 and more than ten acceptor groups) were excluded [19].

128 To understand the possible mechanisms of interaction between substances and  
129 biological targets, we used the SwissTargetPrediction web server [20] to predict the  
130 biological activity of small molecules. The DataWarrior program was employed to  
131 calculate physicochemical properties and analyze molecular scaffolds [21].

## 132 **Preparation of Proteins and Database**

133 X-ray crystal structures of the target proteins were obtained from the Protein Data Bank  
134 (PDB) [22] and used for virtual screening and receptor-oriented docking. Molecules  
135 with properties matching the pharmacophore structure constituting a set of promising  
136 molecules ("hits"), were used in the docking procedure with the active site of the  
137 corresponding target protein.

138 For the *in silico* virtual screening, we used a chemical space of molecules containing  
139 more than 70,000 organic compounds. The compounds of this database (DB\_KSM)  
140 were synthesized by the synthetic group of Prof. S.M. Kovalenko (Department of  
141 Organic Chemistry at Kharkiv National University, Ukraine). They included various  
142 heterocyclic systems with substituents of different electronic nature, including various  
143 aliphatic fragments, amino acid residues, halogens, and others. The representative  
144 structure was cepharanthine (CEP), CAS Number 481-49-2 [23].

## 145 **Molecular Docking**

146 X-ray crystal structures of the corresponding proteins from the Protein Data Bank were  
147 used for docking. Receptor-oriented docking was performed using the AutoDock Vina  
148 program [24].

## 149 **Chemistry**

150 The synthesis of potentially active hit compounds from virtual screening and docking  
151 experiments was carried out using previously developed methods. **Hit2** [25], **Hit3** та  
152 **Hit5** [26], **Hit9**, **Hit10** [27], **Hit13** [28], **Hit7**, **Hit15** [29] were prepared (**Fig. 1**).

153  
154 **Fig 1. Potentially active hits selected as a result of virtual screening and docking**

155  
156 All NMR spectra were recorded on a Varian MR-400 spectrometer with standard pulse  
157 sequences operating at 400 MHz for  $^1\text{H}$  NMR and 101 MHz for  $^{13}\text{C}$  NMR. For all NMR  
158 spectra, DMSO- $d_6$  was used as the solvent. Chemical shift values are referenced to  
159 residual protons ( $\delta_{\text{H}}$  2.49 ppm) and carbons ( $\delta_{\text{C}}$  39.6 ppm) of the solvent as an internal  
160 standard. LC/MS spectra were recorded on an ELSD Alltech 3300 liquid  
161 chromatograph equipped with a UV detector ( $\lambda_{\text{max}}$  254 nm), API-150EX mass-  
162 spectrometer, and using a Zorbax SB-C18 column, Phenomenex (100 × 4 mm) Rapid  
163 Resolution HT cartridge 4.6 × 30 mm, 1.8-Micron. Elution started with 0.1 M solution  
164 of HCOOH in water and ended with 0.1 M solution of HCOOH in acetonitrile, using a  
165 linear gradient at a flow rate of 0.15 mL/min and an analysis cycle time of 25 min.

## 166 ***In vitro* anti-inflammatory activity in human neutrophils**

167 For the *in vitro* studies, the synthesized compounds (**Fig. 1**) were dissolved in dimethyl  
168 sulfoxide (DMSO) to prepare stock solutions. The final concentration of DMSO in cell  
169 experiments did not exceed 0.5% and did not affect the measured parameters. Blood  
170 was taken from healthy human donors using a protocol approved by the Chang Gung  
171 Memorial Hospital review board. Neutrophils were isolated following the standard  
172 procedure [30].

173 The inhibition of superoxide anion generation (respiratory burst) was measured based  
174 on ferricytochrome *c* reduction as previously described [31]. Briefly, preheated  
175 neutrophils ( $6 \times 10^5$  cells·mL<sup>-1</sup>) and 0.6 mg/mL ferricytochrome *c* solution were  
176 treated with the tested compounds or DMSO (control) for 5 min. The cells were  
177 activated with formyl-methionyl-leucyl-phenylalanine (fMLF, 100 nM)/cytochalasin  
178 B (CB, 1 µg/mL) for 13 min. The absorbance was continuously monitored at 550 nm  
179 using Hitachi U-3010 spectrophotometer with constant stirring (Hitachi Inc., Tokyo,  
180 Japan). Calculations were based on the differences in absorbance with and without  
181 superoxide dismutase (SOD, 100 U/mL) divided by the extinction coefficient for the  
182 reduction of ferricytochrome *c* ( $\epsilon = 21.1/\text{mM}/10 \text{ mm}$ ).

183 Elastase release (i.e., degranulation from azurophilic granules) was evaluated as  
184 described before [32]. Briefly, neutrophils were equilibrated with elastase substrate,  
185 MeO-Suc-Ala-Ala-Pro-Val-*p*-nitroanilide (100 µM), at 37 °C for 2 min and then  
186 incubated with the sample for 5 min. Cells were activated by 100 nM fMLF and 0.5  
187 µg/mL CB for 13 min, and changes in the absorbance at 405 nm corresponding to



188 elastase release were continuously monitored. The results were expressed as the  
189 percentage of the initial rate of elastase release in the fMLF/CB-activated drug-free  
190 control system.

## 191 **Pseudotyped lentivirus assay**

192 Lentivirus experiments were approved by the Institutional Biosafety Committee  
193 of Chang Gung University and performed according to our previous report [42]. Stable  
194 hACE-2 overexpressed HEK293T cells were provided by Dr. Rei-Lin Kuo (Chang  
195 Gung University) and maintained in DMEM containing 10 % FBS and 10  $\mu\text{g}/\text{mL}$   
196 blasticidin. VSV-G pseudotyped lentivirus control (clone name: S3w.Fluc.Ppuro) and  
197 SARS-CoV-2 S-protein expressing VSV-G pseudotyped lentiviruses (clone name:  
198 nCoV-S-Luc-D614G and nCoV-S-Luc-B.1.617.2) were purchased from RNAi Core  
199 Facility of Academia Sinica. hACE-2 overexpressed cells ( $1 \times 10^4$  cells/well) were  
200 seeded on 96-well plates and incubated at 37 °C with 5% CO<sub>2</sub>. Equal relative infection  
201 units (RIU) ( $5 \times 10^3$  RIU/well= 0.5 RIU/cell) of pseudotyped lentiviruses were  
202 pretreated with various concentrations of antiviral agents in DMEM containing 5%  
203 FBS at 37 °C for 1 hour. The medium of ACE-2 overexpressed cells was replaced with  
204 treated pseudotyped lentivirus and cultured for 24 h. Luciferase activity was measured  
205 using a Luciferase Assay System (E2520, Promega) and recorded by a Fluorescence  
206 Reader. Cepharanthine served as a positive control.

## 207 **WST-1 viability assay**

208 The potential cytotoxicity of the tested samples was evaluated by the WST-1 reduction  
209 assay in hACE-2-overexpressed HEK293T [40]. The hACE-2-overexpressed  
210 HEK293T cells ( $1 \times 10^4$  cells/well) were preincubated with DMSO or tested agents for  
211 24 h. Then, the WST-1 reagent (M192427, Sigma-Aldrich, MO, USA) was added and  
212 incubated for 4 h at 37 °C. The absorbance at 405 nm was measured by a Multiska GO  
213 spectrophotometer (Thermo Fisher Scientific, MA, USA).

214

## 215 **Statistical analysis**

216 Results are expressed as mean  $\pm$  S.E.M. of two independent measurements  
217 (pseudoviral anti-viral assay) or mean  $\pm$  S.E.M. of three independent measurements  
218 (anti-inflammatory assay). The 50% inhibitory concentration (IC<sub>50</sub>) was calculated  
219 from the dose-response curve obtained by plotting the percentage of inhibition versus  
220 concentrations (linear function, Microsoft Office, anti-inflammatory assay). Statistical  
221 analysis was performed using Student's *t*-test (Sigma Plot, Systat Software, Systat  
222 Software Inc., anti-inflammatory). Values with  $*P < 0.05$ ,  $**P < 0.01$ ,  $***P < 0.001$   
223 were considered statistically significant.

224

## 225 **Results**

### 226 ***In silico* models and calculations**

227 Studies of the bis-benzylisoquinoline alkaloid cepharanthine (CEP) against COVID-  
228 19 identified its significant antiviral and anti-inflammatory potential. However, the

229 precise mechanism of CEP is still under investigation [11, 12]. To model the  
230 mechanism of cepharanthine's action on COVID-19, researchers focused on various  
231 protein targets available in the Protein Data Bank (PDB). According to scientific  
232 literature, one of the primary mechanisms of CEP's action against COVID-19 is its  
233 binding to ACE2, which was validated by molecular dynamics (MD) simulations [33].  
234 Cepharanthine was selected as the representative structure to develop new molecules  
235 with the potential to inhibit key viral pathways. The 3D crystal structure of the receptor  
236 binding domain of the SARS-CoV-2 Omicron variant spike glycoprotein complex with  
237 its receptor, human ACE2 (PDB: 7WBP), was chosen as the biological target.  
238 We conducted a preliminary pharmacophore screening using the LigandScout suite to  
239 identify suitable structures for further investigation. The receptor-binding domain of  
240 the SARS-CoV-2 Omicron spike glycoprotein complex with the human ACE2 receptor  
241 and the ligand NAG PDB 7WBP [34] was employed as a representative protein-ligand  
242 structure for the study (**Fig. 2**).

243  
244 **Fig. 2. Receptor binding domain of SARS-CoV-2 Omicron spike glycoprotein**  
245 **complex with its receptor human ACE2 with ligand NAG (A), the structure of**  
246 **cepharanthine CEP (D) and its pharmacophore (C).**

247  
248 The pharmacophore model CEP was used as a search query to identify compounds  
249 targeting the binding site of the biological target. Virtual screening (VS) of a molecular  
250 database (DB\_KSM) according to the pharmacophore identified in the previous step

251 resulted in identifying several compounds that could be promising in the fight against  
252 COVID-19. Based on matching with the pharmacophore, 23 compounds were selected  
253 for further study (**Fig. 3**).

254

255 **Fig 3. The structures with possible activity against SARS-COV2 according to VS**  
256 **results of DB\_KSM database.**

257

258 The docking of these molecules to the receptor-binding domain of the SARS-CoV-2  
259 Omicron spike glycoprotein complex with the human ACE2 receptor (PDB 7WBP)  
260 was performed. Their binding affinity parameters were calculated. The binding affinity  
261 scores (BAS) and binding energies (BE, kcal/mol) of the docked hit compounds, along  
262 with the co-crystallized ligand (NAG) and CEP, are presented in **Table 1**.

263 **Table 1. Affinity parameters of hit structures (complex PDB 7WBP)**

Mol	BAS	BE (kcal/mol)	Mol	BAS	BE (kcal/mol)
NAG	-2.04	-7.10	CEP	-17,54	-7,30
<b>Hit1</b>	<b>-6,93</b>	<b>-6,60</b>	<b>Hit13</b>	<b>-17.71</b>	<b>-9.10</b>
<b>Hit2</b>	<b>-11.14</b>	<b>-8.50</b>	<b>Hit14</b>	<b>-6,88</b>	<b>-6,50</b>
<b>Hit3</b>	<b>-15.91</b>	<b>-7.90</b>	<b>Hit15</b>	<b>-10.14</b>	<b>-9.10</b>
<b>Hit4</b>	<b>-6,78</b>	<b>-7,10</b>	<b>Hit16</b>	<b>-6,56</b>	<b>-7,10</b>
<b>Hit5</b>	<b>-12.41</b>	<b>-7.60</b>	<b>Hit17</b>	<b>-6,38</b>	<b>-6,90</b>
<b>Hit6</b>	<b>-5,86</b>	<b>-7,00</b>	<b>Hit18</b>	<b>-5,85</b>	<b>-6,70</b>
<b>Hit7</b>	<b>-7.56</b>	<b>-8.60</b>	<b>Hit19</b>	<b>-5,49</b>	<b>-6,80</b>
<b>Hit8</b>	<b>-7,00</b>	<b>-6,90</b>	<b>Hit20</b>	<b>-7,13</b>	<b>-7,00</b>

<b>Hit9</b>	<b>-10.78</b>	<b>-8.50</b>	<b>Hit21</b>	-6,67	-6,56
<b>Hit10</b>	<b>-13.89</b>	<b>-8.40</b>	<b>Hit22</b>	-2,54	-6,10
<b>Hit11</b>	-6,48	-6,90	<b>Hit23</b>	-4,34	-5,85
<b>Hit12</b>	-5,26	-7,00			

264

265 As shown in **Table 1**, eight compounds (**Hit2**, **Hit3**, **Hit5**, **Hit7**, **Hit9**, **Hit10**, **Hit13**,  
266 and **Hit15**) exhibited binding energies exceeding the absolute values of the  
267 representative cepharanthine (CEP) structure. These compounds were selected for  
268 further molecular docking studies with target proteins identified in the literature as  
269 potential pharmacological targets of cepharanthine [33].

270 For the calculations, hub targets for the potential pharmacological mechanism of CEP  
271 against COVID-19 were selected (**Table 2**). In the study [33], "network pharmacology"  
272 combined with RNA sequencing, molecular docking, and MD modeling was used to  
273 identify hub targets and potential pharmacological mechanisms of cepharanthine  
274 (CEP) against COVID-19. Nine key hub genes (ACE2, STAT1, SRC, PIK3R1, HIF1A,  
275 ESR1, ERBB2, CDC42, and BCL2L1) were identified. Based on these data, we  
276 performed docking studies of the home library to the hub targets from the Protein Data  
277 Bank [22] described above.

278

279 **Table 2. Hub-targets and potential pharmacological mechanisms of action of**  
280 **cepharanthine (CEP) against COVID-19**

<b>Target</b>	<b>Designation</b>	<b>Classification</b>
---------------	--------------------	-----------------------

<b>1BF5</b>	Tyrosine phosphorylated STAT-1/DNA complex	Gene regulation/DNA
<b>1A07</b>	C-SRC (SH2 domain) complexed with acemalonyl tyr-glu-(N,N-dipentyl amine)	Complex (transferase/peptide)
<b>2IUI</b>	Crystal structure of the PI3-kinase p85 N-terminal SH2 domain in complex with PDGFR phosphotyrosyl peptide	Transferase
<b>1H2K</b>	Factor Inhibiting HIF-1 alpha in complex with HIF-1 alpha fragment peptide	Transcription activator/inhibitor
<b>2AJF</b>	Structure of SARS coronavirus spike receptor-binding domain complexed with its receptor	Hydrolase / viral protein
<b>1A52</b>	Estrogen receptor alpha ligand-binding domain complexed to estradiol	Receptor
<b>2A91</b>	Crystal structure of ErbB2 domains 1-3	Signaling protein, transferase, membrane protein
<b>7S0Y</b>	Structures of TcdB in complex with Cdc42	Hydrolase
<b>7JGW</b>	Crystal structure of BCL-XL in complex with compound 1620116, crystal form 1	Apoptosis

281

282 Docking was performed using AutoDock Vina with CEP and the studied molecules.

283 The results of molecular docking and binding energies of the molecules are presented

284 in **Table 3**.

285

286 **Table 3. Molecular docking binding energy results of hub genes with CEP and**

287 **hit-molecules**

Target	REF <sup>a</sup>	CEP <sup>a</sup>	Hit2	Hit3	Hit5	Hit7	Hit9	Hit10	Hit13	Hit15
--------	------------------	------------------	------	------	------	------	------	-------	-------	-------

1BF5	-6.0	-9.8	-9.1	-8.7	-9.3	-8.9	-9.0	-9.0	-8.7	-8.9
1A07	-7.0	-7.4	-8.1	-7.0	-8.3	-7.3	-8.8	-7.2	-8.2	-7.6
2IUI	-6.2	-9.5	-9.2	-9.3	-9.8	-8.7	-9.2	-8.9	-9.2	-8.2
1H2K	-4.3	-8.8	-8.1	-9.2	-8.4	-8.0	-8.9	-7.9	-8.6	-8.0
2AJF	<b>-5.6</b>	<b>-11.1</b>	<b>-9.7</b>	<b>-9.3</b>	<b>-9.2</b>	<b>-8.8</b>	<b>-10.0</b>	<b>-8.7</b>	<b>-9.6</b>	<b>-9.0</b>
1A52	-10.4	-8.2	-9.3	-8.4	-10.1	-8.2	-9.2	-9.4	-9.4	-8.7
2A91	-6	-9.7	-9.8	-8.4	-8.2	-8.9	-10.0	-8.8	-8.9	-8.2
7S0Y	-6.7	-8.3	-9.4	-8.1	-8.5	-9.5	-8.4	-9.1	-8.7	-7.4
7JGW	-10.4	-8.9	-8.9	-7.6	-8.5	-8.2	-8.4	-9.5	-9.2	-8.6

288 <sup>a</sup> Data from [33]

289

290 The molecular docking results showed a good potential for inhibition of Target 2AJF,  
291 the spike receptor-binding domain of SARS-CoV-2, in complex with its receptor and  
292 a set of targets responsible for modulating the immune response.

293 Additionally, we utilized the SwissTargetPrediction resource further to evaluate the  
294 most likely macromolecular targets for CEP (**Fig. 4**) and the new molecules to assess  
295 the possibility of using multiple therapeutically relevant targets for the studied  
296 compounds, as most bioactive molecules have more than one target [35].

297

298 **Fig 4. The most probable macromolecular targets of CEP, suggested by the**  
299 **SwissTargetPrediction resource [20]**

300

301 The identified biological targets for CEP included the family A G protein-coupled  
302 receptors – cell surface proteins that detect molecules outside the cell and activate

303 cellular responses, including immune responses. They also included the  
304 electrochemical transporters and ligand-gated ion channels responsible for signal  
305 molecule transport regulated by membrane potential or ion flow. The biological targets  
306 of the new hit compounds are presented as an aggregate bar chart (**Fig. 5**), reflecting  
307 the contribution of each category.

308 **Fig 5. Biological target pool of the new hit molecules proposed by the**  
309 **SwissTargetPrediction resource [20]**

310  
311 The primary predicted target categories for the new hit molecules, as proposed by the  
312 SwissTargetPrediction resource, were the kinase/family A G / B G protein-coupled  
313 receptors/protease.

314 **Table 4** presents the categories of biological targets for the new hit molecules: a)  
315 Targets responsible for modulating the immune response, which may be one of the  
316 mechanisms contributing to tissue inflammation in COVID-19 (kinases  
317 (phosphotransferases) / protein-coupled receptor A G /B G family); b) Targets from  
318 the protease category, which may be involved in inhibiting key pathways of viral  
319 replication.

320  
321 **Table 4. Categories of biological targets for pharmacological action against**  
322 **SARS-COV-2 used in the study**

Target	Designation	Classification
--------	-------------	----------------



4E4L	AK1 kinase (JH1 domain) in complex	Transferase/kinase
4D1S	Crystal structure of JAK2 kinase	Transferase/kinase
4Z16	Crystal Structure of the Jak3 Kinase Domain	Transferase/kinase
1ALU	Human Interleukin-6	Cytokine
7WOF	Crystal structure of SARS-CoV-2 Mpro	Viral protein/protease
7LLZ	Crystal structure of SARS-CoV-2 papain-like protease (PLpro)	Viral protein/protease

323  
324 The results of the molecular docking, the energy characteristics of the binding affinity  
325 in kcal/mol (A), and the binding affinity score (BAS) of the studied molecules for the  
326 main predicted categories of biological targets are presented in **Table 5**.

327  
328 **Table 5. Results of molecular docking: Energy characteristics of binding affinity**  
329 **in kcal/mol (A) and binding affinity score (BAS) of the studied molecules for the**  
330 **main predicted categories of biological targets**

Biological targets		Ligand	Hit2	Hit3	Hit5	Hit7	Hit9	Hit10	Hit13	Hit15	CEP
4E4L	A	-11.0	-5.8	-6.9	-6.8	-8.4	-6.5	-6.4	-8.3	-6.3	-5.9
	BAS	-18.4	-14.1	-13.0	-13.6	-21.7	-29.0	-28.4	-13.8	-16.4	-10.7
4D1S	A	-10.7	-8.4	-9.6	-9.3	-9.5	-9.5	-9.5	-8.5	-9.4	-5.5
	BAS	-13.7	-14.6	-14.3	-11.0	-14.4	-17.6	-18.9	-6.2	-2.3	-10.6
4Z16	A	-8.2	-8.7	-9.5	-9.0	-6.9	-9.8	-9.4	-9.3	-9.2	-10.4
	BAS	-10.9	-18.3	-12.1	-14.7	-12.4	-13.9	-12.5	-13.3	-10.2	-10.6
1ALU	A	-4.6	-5.1	-5.9	-6.1	-6.0	-5.8	-6.1	-6.9	-5.7	-4.5
	BAS	-12,5	-2.1	-16.8	-7.6	-15.3	-2.1	-3.2	-7.9	-1.0	-2.0

<b>7WOF</b>	<b>A</b>	-6.8	-6.4	-6.3	-6.7	-7.1	-7.6	-7.6	-7.7	-7.9	-4.9
	<b>BAS</b>	-14.6	-10.5	-8.8	-13.5	-6.5	-8.8	-5.4	-1.4	-13.6	9.3
<b>7LLZ</b>	<b>A</b>	-8.9	-7.8	-8.1	-8.5	-8.8	-8.0	-8.0	-8.4	-7.9	-7.3
	<b>BAS</b>	-20.0	-12.5	-1.1	-12.5	-16.7	-3.9	-7.3	-7.4	-13.2	-15.2

331  
 332 The tested molecules showed potential inhibition of Target 4Z16 (Jak3), a domain of  
 333 the Janus kinase JAK3, a representative of tyrosine kinases, cytoplasmic enzymes  
 334 involved in mediating intracellular signaling from cytokine receptors, which are  
 335 responsible for inflammation processes [36]. Hit molecules also showed potential  
 336 inhibition of SARS-COV-2 proteases Mpro and PLpro.  
 337 Several ADME parameters were calculated to evaluate the suitability of the identified  
 338 compounds in terms of drug-like properties, including chemical absorption,  
 339 distribution, metabolism, and excretion, which play a crucial role in determining  
 340 potential drug molecules. **Table 6** presents parameters such as lipophilicity (clogP),  
 341 topological polar surface area (TPSA), molecular weight (parameter SIZE, g/mol),  
 342 solubility (LogS), fraction of sp<sup>3</sup> carbon atoms (Fraction Csp<sup>3</sup>), flexibility, and optimal  
 343 values of these parameters. The studied molecules conform to the drug-likeness  
 344 properties.

345

346 **Table 6. Drug-likeness properties of selected hits**

<b>Name</b>	<b>Log P<sub>ow</sub></b>	<b>SIZE (g/mol)</b>	<b>TPSA, Å<sup>2</sup></b>	<b>LogS</b>	<b>Fraction C (sp<sup>3</sup>)</b>	<b>Flexibility</b>
	<i>-0.7 &lt; X &lt; 5.0</i>	<i>150 &lt; X &lt; 500</i>	<i>20 &lt; X &lt; 130</i>	<i>0 &lt; -X &lt; 6</i>	<i>0.25 &lt; X &lt; 1</i>	<i>0 &lt; X &lt; 9</i>
<b>Hit2</b>	3.51	504.60	121.65	-4.82	0.26	12

<b>Hit3</b>	5.09	442.51	90.02	-5.71	0.23	9
<b>Hit5</b>	4.35	462.93	90.02	-6.00	0.20	9
<b>Hit7</b>	5.00	389.47	97.34	-5.72	0.14	5
<b>Hit9</b>	3.74	438.48	137.16	-4.98	0.14	7
<b>Hit10</b>	3.61	450.51	116.39	-4.89	0.18	8
<b>Hit13</b>	1.97	435.41	122.28	-3.70	0.09	9
<b>Hit15</b>	3.22	473.57	151.90	-4.63	0.25	9

347

348 ***In vitro* models**

349 **SARS-CoV-2 spike/ACE2 pseudovirus neutralization assay**

350 The S-protein and ACE2 receptor play an essential role in the early phases of  
351 coronavirus infection [37]. The established binding assay is based on measuring  
352 luciferase activity and utilizes stable hACE-2 overexpressed HEK293T cells and  
353 SARS-CoV-2 S-protein expressing VSV-G pseudotyped lentiviruses. Omicron  
354 B.1.1.529 SARS-CoV-2 coronavirus subtype was chosen as the most related subtype to  
355 the current variant. It is well known that the mutations increase the infectivity of the  
356 COVID-19 virus [38]. The cytotoxicity against hACE2-293T cells was tested, and the  
357 results revealed no toxicity (**Table 7**).

358

359 **Table 7. Effects of synthetic compounds on hACE-2 overexpressed HEK293T**  
360 **viability**

<b>Compound</b>	<b>Cell viability (%)<sup>a</sup></b>
<b>Hit13</b>	105.92

<b>Hit9</b>	103.83
<b>Hit3</b>	95.82
<b>Hit 7</b>	99.47
<b>Hit10</b>	96.57
<b>Hit5</b>	95.19
<b>Hit15</b>	97.33
<b>Hit2</b>	100.00

361 <sup>a</sup> Percentage of cell at 10  $\mu$ V(n = 1). Control group (DMSO)

362 Next, the SARS-CoV-2 S-protein and ACE2 binding assay results showed activity of  
363 **Hit15** with 43.0% inhibition at 10  $\mu$ M (**Table 8**). The compound possesses sulfonyl  
364 and pyrimidone moiety that may be responsible for the observed activity [39, 40].

365

366 **Table 8. Effect of synthetic compounds in the pseudovirus neutralization assay of**  
367 **Omicron variants (SARS-CoV-2 Spike protein pseudotyped lentivirus type).**

<b>Compound</b>	<b>Inh%<sup>a</sup></b>
<b>Hit13</b>	19.78 $\pm$ 8.29
<b>Hit9</b>	2.14 $\pm$ 10.15
<b>Hit3</b>	10.46 $\pm$ 5.69
<b>Hit 7</b>	22.12 $\pm$ 14.37
<b>Hit10</b>	14.25 $\pm$ 9.76
<b>Hit5</b>	0.08 $\pm$ 6.23
<b>Hit15</b>	43.00 $\pm$ 0.80
<b>Hit2</b>	29.56 $\pm$ 13.34
<b>Cepharanthine</b>	97.33 $\pm$ 0.08

368 <sup>a</sup> Percentage of inhibition (Inh.%) at 10  $\mu$ M. Results are presented as mean  $\pm$  S.E.M. (n = 2). Control  
369 group (DMSO). SARS-CoV-2 pseudovirus strain: Omicron (B.1.1.529).

370

371 In the pseudovirus neutralization assay, cepharanthine showed 97.3% inhibition  
372 at 10  $\mu$ M and IC<sub>50</sub> 1.07  $\pm$  0.24  $\mu$ M. The antiviral potential of HIT15 and cepharanthine  
373 were in agreement with the reported data [41] . They indicated that both compounds  
374 may suppress infection of SARS-CoV-2 pseudovirus in hACE2-overexpressed host  
375 cells and may interfere with the S-protein/ACE2 binding. Previous research suggested  
376 that reducing the activity of TMPRSS2 using plant secondary metabolites could help  
377 manage COVID-19. TMPRSS2 is crucial for the virus entry stage by priming the  
378 S-protein of SARS-CoV-2, which facilitates the fusion of viral and host cell  
379 membranes. In an *in vitro* molecular docking study, cepharanthine interacted well with  
380 the TMPRSS2 and SARS-CoV-2 S-protein [43]. These data bode well with the docking  
381 result for cepharantine (**Table 3**) in the SARS-CoV-2 S-protein/ACE2 binding pocket.  
382 The anti-inflammatory activity was studied *in vitro* in a model of inhibition of  
383 superoxide anion release and elastase in human neutrophils. The effect of new  
384 molecules on superoxide anion generation and elastase release in activated human  
385 neutrophils was studied (**Table 9**). Superoxide anion generation and elastase release  
386 were induced by FMLP/CB and measured respectively. All data are expressed as mean  
387  $\pm$  S.E.M. (n = 3–4). \**P* < 0.05, \*\**P* < 0.01, and \*\*\**P* < 0.001 compared with the  
388 control.

389

390 **Table 9. Effects of compounds on superoxide anion generation and elastase release**  
391 **in fMLF/CB-induced human neutrophils**

Compound	Superoxide anion			Elastase release		
	IC <sub>50</sub> (μM) <sup>a</sup>	Inh%		IC <sub>50</sub> (μM) <sup>a</sup>	Inh%	
<b>Hit13<sup>b</sup></b>	> 100	-4.72 ± 6.46		19.73 ± 2.39	113.52 ± 8.51	***
<b>Hit9<sup>b</sup></b>	> 100	-0.55 ± 0.96		17.12 ± 0.19	122.94 ± 5.95	***
<b>Hit10<sup>b</sup></b>	> 100	-0.40 ± 2.56		18.78 ± 4.25	73.21 ± 5.87	***
<b>Hit15<sup>b</sup></b>	1.43 ± 0.18	100.41 ± 0.28	***	1.28 ± 0.33	114.63 ± 1.32	***
<b>Hit5<sup>c</sup></b>	> 50	0.02 ± 1.67		> 50	26.06 ± 3.28	**
<b>Hit3<sup>d</sup></b>	> 10	-0.61 ± 0.43		> 10	22.11 ± 6.04	*
<b>Hit7<sup>d</sup></b>	> 10	7.19 ± 2.87		> 10	34.27 ± 2.90	***
<b>Hit2<sup>d</sup></b>	> 10	5.99 ± 2.80		> 10	7.60 ± 4.78	***
LY294002 <sup>e</sup>	1.76 ± 0.28	96.14 ± 1.79	***	2.23 ± 0.15	84.59 ± 2.86	***

Results are presented as mean ± S.E.M. (n = 3). \**P* < 0.05, \*\**P* < 0.01, \*\*\**P* < 0.001 compared with the control (DMSO).

<sup>a</sup> Concentration necessary for 50% inhibition (IC<sub>50</sub>).

<sup>b</sup> Percentage of inhibition (Inh%) at 100 μM. Compounds' solubility was 50 mM.

<sup>c</sup> Percentage of inhibition (Inh%) at 50 μM. Compound solubility was 25 mM.

<sup>d</sup> Percentage of inhibition (Inh%) at 10 μM. Compounds' solubility is 5 mM.

<sup>e</sup> Positive control.

392  
393 Experimental results showed that **Hit13**, **Hit9**, and **Hit10** moderately affected elastase  
394 release. **Hit15** showed good anti-inflammatory activity with IC<sub>50</sub> 1.76 and 2.23 μM in  
395 both superoxide anion generation and elastase release assays in fMLF/CB-induced  
396 human neutrophils, respectively. The **Hit15** molecule has good potential for further  
397 development to treat COVID-19.

398

## 399 CONCLUSION

400 A virtual *in silico* screening and receptor-oriented docking was conducted on three-  
401 dimensional structural models of active sites in biological molecules involved in the  
402 mechanisms of SARS-CoV-2 impact on the body, using cepharanthine as a  
403 representative structure. Several hit molecules were identified, characterized by  
404 binding energies with the active sites of the targets at levels comparable to or exceeding  
405 those of the representative cepharanthine structure. Receptor-oriented docking  
406 revealed that these hit molecules have the potential to inhibit SARS-CoV-2 proteases  
407 Mpro and PLpro, which play a crucial role in viral replication mechanisms, as well as  
408 to inhibit Janus kinase (Jak3), which mediates intracellular signal transduction and is  
409 responsible for inflammatory processes.

410 The hit molecules were evaluated *in vitro* for anti-inflammatory activity. They were  
411 demonstrated by assessing their inhibitory effects on elastase release in human  
412 neutrophils and the generation of superoxide anions, a characteristic of anti-  
413 inflammatory action. It was shown that the 2-((5-((4-isopropylphenyl)sulfonyl)-6-oxo-  
414 1,6-dihydropyrimidin-2-yl)thio)-N-(3-methoxyphenyl)acetamide (**Hit15**) exhibited  
415 potent anti-inflammatory activity. Several other molecules also demonstrated moderate  
416 effects on elastase release.

417

### 418 Author Contributions

419 V.A.G., V.V.I. - Conceptualization,

420 Y.-L.C., S.-Y.F., L.V.Y., O.M.K. - Data Curation

421 V.A.G, O.M.K. - Project Administration

422 V.V.I., A.B.Z., D.O.A. - Software

423 O.M.K., T.-L.H. - Supervision.

424 L.V.Y., V.V.I., S.M.K., M.E.-S., M.K., O.O.M. - Writing – original draft

425 V.A.G. – Writing - Review & Editing;

426 T.-L.H., O.M.K. - Funding Acquisition

427 All authors have read and agreed to the published version of the manuscript.

428

## 429 **Acknowledgement**

430 VVI, ABZ, SMK, L.V.Y and O.M.K. express their gratitude to the National  
431 Research Foundation of Ukraine ([https://nrfu.org.ua/en/fundraising\\_en/](https://nrfu.org.ua/en/fundraising_en/)) for financial  
432 support (grant No. 87/0062 (2021.01/0062) “Molecular design, synthesis and screening  
433 of new potential antiviral pharmaceutical ingredients for the treatment of infectious  
434 diseases COVID-19”). This research was supported by grants from the National  
435 Science and Technology Council (<https://www.nstc.gov.tw>) (NSTC 113-2321-B-255-  
436 001, 113-2321-B-182-003, 112-2321-B-182-003, 112-2321-B-255-001, 111-2320-B-  
437 255-006-MY3, and 111-2321-B-255-001 granted to T.L.H.; and 113-2320-B-037-023,  
438 112-2320-B-037-012, and 111-2320-B-037-007 granted to M.K.), Chang Gung  
439 University of Science and Technology (<https://english.cgust.edu.tw>) (ZRRPF3L0091  
440 and ZRRPF3N0101) granted to T.L.H., Chang Gung Memorial Hospital  
441 (<https://www.cgmh.org.tw/eng>) (CMRPF1P0051-3, CMRPF1P0071-3) granted to



442 T.L.H., and Kaohsiung Medical University Research Foundation  
443 (<https://www.kmu.edu.tw/index.php/en-gb/research>) (KMU-Q113011) granted to  
444 M.K., Taiwan. We thank Prof. T. Langer for the opportunity to work with the  
445 LigandScout suite.

446 The funders had no role in the study design, data collection, analyses, decision  
447 to publish, or manuscript preparation.

448

#### 449 **Institutional Review Board Statement**

450 The study was conducted according to the guidelines of the Declaration of Helsinki  
451 and approved by the Institutional Review Board of Chang Gung Memorial Hospital  
452 (Registration number: IRB No.: 202301906A3C501), 1<sup>st</sup> August to 30<sup>th</sup> September  
453 2024 was the recruitment period for this study.

454

#### 455 **Informed Consent Statement**

456 Informed consent written and signed by donors was obtained from all subjects involved  
457 in the study. No minors were included.

458

#### 459 **Data Availability Statement**

460 All data are fully available without restriction. All relevant data are within the  
461 manuscript.

462

#### 463 **Conflicts of Interest**

464 There are no competing interests to declare.

## 466 **References**

- 467 1. World Health Organization. (2020). Corticosteroids for COVID-19. WHO-  
468 2019-nCoV-Corticosteroids-2020.1-eng.pdf.  
469 [https://iris.who.int/bitstream/handle/10665/334125/WHO-2019-nCoV-](https://iris.who.int/bitstream/handle/10665/334125/WHO-2019-nCoV-Corticosteroids-2020.1-eng.pdf?sequence=1)  
470 [Corticosteroids-2020.1-eng.pdf?sequence=1](https://iris.who.int/bitstream/handle/10665/334125/WHO-2019-nCoV-Corticosteroids-2020.1-eng.pdf?sequence=1).
- 471 2. Inpatient Considerations in COVID-19 Treatment and Prevention. *US*  
472 *Pharm.* 2022;47(4):HS-1-HS-7.
- 473 3. Zagaliotis P, Petrou A, Mystridis GA, Geronikaki A, Vizirianakis IS, Walsh TJ.  
474 Developing New Treatments for COVID-19 through Dual-Action  
475 Antiviral/Anti-Inflammatory Small Molecules and Physiologically Based  
476 Pharmacokinetic Modeling. *Int J Mol Sci.* 2022 Jul 20;23(14):8006. doi:  
477 10.3390/ijms23148006. PMID: 35887353; PMCID: PMC9325261.
- 478 4. Ramesh S, Govindarajulu M, Parise RS, Neel L, Shankar T, Patel S. Emerging  
479 SARS-CoV-2 Variants: A Review of Its Mutations, Its Implications and  
480 Vaccine Efficacy. *Vaccines (Basel).* 2021 Oct 18;9(10):1195. doi:  
481 10.3390/vaccines9101195. PMID: 34696303; PMCID: PMC8537675
- 482 5. Aleem A, Akbar Samad AB, Vaqar S. Emerging Variants of SARS-CoV-2 and  
483 Novel Therapeutics Against Coronavirus (COVID-19). 2023 May 8. In:  
484 StatPearls [Internet]. Treasure Island (FL): StatPearls Publishing; 2024 Jan–.  
485 PMID: 34033342.
- 486 6. World Health Organization. (2020). Clinical care for severe acute respiratory  
487 infection: toolkit: COVID-19 adaptation. World Health Organization.

- 488 <https://iris.who.int/bitstream/handle/10665/331736/WHO-2019-nCoV->  
489 [SARI\\_toolkit-2020.1-eng.pdf](#)
- 490 7. Rohilla S. Designing therapeutic strategies to combat severe acute respiratory  
491 syndrome coronavirus-2 disease: COVID-19. *Drug Dev Res.* 2021;82:12–26
- 492 8. Lai KH, Chen YL, Lin MF, El-Shazly M, Chang YC, Chen PJ. *Lonicerae*  
493 *Japonicae Flos Attenuates Neutrophilic Inflammation by Inhibiting Oxidative*  
494 *Stress. Antioxidants (Basel).* 2022 Sep 9;11(9):1781. doi:  
495 [10.3390/antiox11091781](https://doi.org/10.3390/antiox11091781). PMID: 36139855; PMCID: PMC9495740
- 496 9. Li J, Zhang K, Zhang, y. *et al.* Neutrophils in COVID-19: recent insights and  
497 advances. *Virology* **20**, 169 (2023). [https://doi.org/10.1186/s12985-023-02116-](https://doi.org/10.1186/s12985-023-02116-w/)  
498 [w/](#)
- 499 10. Anti-inflammatory, antiallergic and COVID-19 protease inhibitory activities of  
500 phytochemicals from the Jordanian hawksbeard: identification, structure–  
501 activity relationships, molecular modeling and impact on its folk medicinal  
502 uses. *RSC Adv.*, 2020,10, 38128-38141.  
503 <https://pubs.rsc.org/en/content/articlelanding/2020/ra/d0ra04876c>
- 504 11. Fan H, He ST, Han P, Hong B, Liu K, Li M, Wang S, Tong Y. Cepharranthine:  
505 A Promising Old Drug against SARS-CoV-2. *Adv Biol (Weinh).* 2022  
506 Dec;6(12):e2200148. doi: 10.1002/adbi.202200148. Epub 2022 Jul 1. PMID:  
507 35775953; PMCID: PMC9350037
- 508 12. Xia B, Zheng L, Li Y, Sun W, Liu Y, Li L, Pang J, Chen J, Li J, Cheng H. The  
509 brief overview, antiviral and anti-SARS-CoV-2 activity, quantitative methods,  
510 and pharmacokinetics of cepharanthine: a potential small-molecule drug against

- 511 COVID-19. *Front Pharmacol.* 2023 Jul 31;14:1098972. doi:  
512 10.3389/fphar.2023.1098972. PMID: 37583901; PMCID: PMC10423819
- 513 13.Lengauer T, Rarey M. Computational methods for biomolecular docking.  
514 *Current Opinion in Structural Biology*, Jun 1996, 6 (3): 402–6.  
515 doi:10.1016/S0959-440X(96)80061-3. PMID 8804827
- 516 14.Ivanov VV, Lohachova KO, Kolesnik YV, Zakharov AB, Yevsieieva L V,  
517 Kyrychenko AV, Langer T, Kovalenko SM, Kalugin ON. Recent advances in  
518 computational drug discovery for therapy against coronavirus SARS-CoV-2.  
519 *ScienceRise: Pharmaceutical Science*, 2023, DOI: 10.15587/2519-  
520 4852.2023.290318
- 521 15.Jmol: an open-source Java viewer for chemical structures in 3D. Available  
522 from: <http://www.jmol.org/>
- 523 16.DeLano WL. Pymol: An open-source molecular graphics tool. *CCP4*  
524 *Newsletter On Protein Crystallography* 2002, 40: 82–92
- 525 17.Wolber G, Dornhofer AA, Langer T. Efficient overlay of small organic  
526 molecules using 3D pharmacophores. *J. Comput.-Aided Mol. Des.* 2006, 20  
527 (12): 773–788. <https://doi.org/10.1007/s10822-006-9078-7>
- 528 18.LigandScout. Available from: <https://www.inteligand.com/ligandscout/>
- 529 19.Lipinski CA, Lombardo F, Dominy BW, Feeney PJ. Experimental and  
530 computational approaches to estimate solubility and permeability in drug  
531 discovery and development settings. *Adv. Drug Deliv. Rev.*, 2012, 64: 4–17,  
532 doi: 10.1016/j.addr.2012.09.019.
- 533 20.SwissTargetPrediction. Available from: <http://swisstargetprediction.ch/>.

- 534 21.DataWarrior. Available from: <https://openmolecules.org/datawarrior/>
- 535 22.Protein Data Bank, Database [Internet]. Available from: [www.rcsb.org](http://www.rcsb.org)
- 536 23.Cepharanthine. PubChem, Database [Internet]. Available from:
- 537 <https://pubchem.ncbi.nlm.nih.gov/compound/10206>
- 538 24.AutoDock Vina. Available from: [https://autodock-](https://autodock-vina.readthedocs.io/en/latest/docking_basic.html)
- 539 [vina.readthedocs.io/en/latest/docking\\_basic.html](https://autodock-vina.readthedocs.io/en/latest/docking_basic.html)
- 540 25.Tkachenko OV, Vlasov SV, Kovalenko SM, Zhuravel IO, Chernykh VP.
- 541 Synthesis and the antimicrobial activity of 1-N-alkylated derivatives of 3-N-
- 542 substituted 1H-thieno[3,2-d]pyrimidine-2,4-diones. Journal of Organic and
- 543 Pharmaceutical Chemistry. 2013, 11(4): 15-21.
- 544 26.Kharchenko YV, Detistov AS, Orlov VD. Polycyclic systems containing 1,2,4-
- 545 oxadiazole ring. 3. 3-(1,2,4-oxadiazol-5-yl)pyridin-2(1H)-ones-synthesis and
- 546 prediction of biological activity. Visnik Kharkivs'kogo Natsional'nogo
- 547 Universitetu im. V. N. Karazina. 2008; 820: 216-224.
- 548 27.Borisov AV, Detistov OS, Pukhovaya VI, Zhuravel' IO, Kovalenko SM.
- 549 Parallel liquid-phase synthesis of 5-(1H-4-pyrazolyl)-[1,2,4]oxadiazole
- 550 libraries. J Comb Chem. 2009 Nov-Dec;11(6):1023-9. doi:
- 551 10.1021/cc900070m. PMID: 19711964.
- 552 28.Konovalova IS, Geleverya AO, Kovalenko SM, Reiss GJ. One-pot synthesis
- 553 and crystal structure of diethyl 2,6-dimethyl-4-(1-(2-nitrophenyl)-1H-1,2,3-
- 554 triazol-4-yl)-1,4-dihydropyridine-3,5-dicarboxylate, C<sub>21</sub>H<sub>23</sub>N<sub>5</sub>O<sub>6</sub>. Zeitschrift
- 555 für Kristallographie - New Crystal Structures. 2023; 2 (238): 381-384.
- 556 <https://doi.org/10.1515/ncrs-2022-0573>

- 557 29.Vlasov SV, Kovalenko SM, Chernykh VP, Krolenko KY. Synthesis of 5-  
558 methyl-4-thio-6-(1,3,4-oxadiazol-2-yl)thieno[2,3-d]pyrimidines and their  
559 antimicrobial activity study. Journal of Chemical and Pharmaceutical Research.  
560 2014; 6(6): 22-27.
- 561 30.Boyum A. Isolation of mononuclear cells and granulocytes from human blood.  
562 Isolation of monuclear cells by one centrifugation, and of granulocytes by  
563 combining centrifugation and sedimentation at 1 g. Scand J Clin Lab Invest  
564 Suppl. 1968; 97: 77-89.
- 565 31.Korinek M, Hsieh PS, Chen YL, Hsieh PW, Chang SH, Wu YH, Hwang TL.  
566 Randialic acid B and tomentosolic acid block formyl peptide receptor 1 in  
567 human neutrophils and attenuate psoriasis-like inflammation in vivo. Biochem  
568 Pharmacol. 2021; 190:114596.
- 569 32.Tsai YF, Chu TC, Chang WY, Wu YC, Chang FR, Yang SC, Wu TY, Hsu YM,  
570 Chen CY, Chang SH, Hwang TL. 6-Hydroxy-5,7-dimethoxy-flavone  
571 suppresses the neutrophil respiratory burst via selective PDE4 inhibition to  
572 ameliorate acute lung injury. Free Radic Biol Med. 2017;106: 379-392.
- 573 33.Liu J, Sun T, Liu S, Liu J, Fang S, Tan S, Zeng Y, Zhang B, Li W. Dissecting  
574 the molecular mechanism of cepharanthine against COVID-19, based on a  
575 network pharmacology strategy combined with RNA-sequencing analysis,  
576 molecular docking, and molecular dynamics simulation. Comput Biol Med.  
577 2022 Dec;151(Pt A):106298. doi: 10.1016/j.combiomed.2022.106298. Epub  
578 2022 Nov 11. PMID: 36403355; PMCID: PMC9671524.

- 579 34.PDB 7WBP. Database [Internet]. Available from:  
580 <https://www.rcsb.org/structure/7WBP>
- 581 35.Gfeller D, Michielin O, Zoete V. Shaping the interaction landscape of bioactive  
582 molecules. *Bioinformatics*. 2013 Dec 1;29(23):3073-9. doi:  
583 10.1093/bioinformatics/btt540. Epub 2013 Sep 17. PMID: 24048355.
- 584 36.Tanaka Y, Luo Y, O'Shea JJ, Nakayamada S. Janus kinase-targeting therapies  
585 in rheumatology: a mechanisms-based approach. *Nat Rev Rheumatol*. 2022  
586 Mar;18(3):133-145. doi: 10.1038/s41584-021-00726-8. Epub 2022 Jan 5.  
587 PMID: 34987201; PMCID: PMC8730299.
- 588 37.Hoffmann M, Kleine-Weber H, Schroeder S, Krüger N, Herrler T, Erichsen S  
589 et al. SARS-CoV-2 Cell Entry Depends on ACE2 and TMPRSS2 and Is  
590 Blocked by a Clinically Proven Protease Inhibitor. *Cell*. 2020 Apr  
591 16;181(2):271-280.e8. doi: 10.1016/j.cell.2020.02.052. Epub 2020 Mar 5.  
592 PMID: 32142651; PMCID: PMC7102627.
- 593 38.Korber B, Fischer WM, Gnanakaran S, et al. Tracking Changes in SARS-  
594 CoV-2 Spike: Evidence that D614G Increases Infectivity of the COVID-19  
595 Virus. *Cell*. 2020/08/20/ 2020;182(4):812-827.e19.  
596 doi:<https://doi.org/10.1016/j.cell.2020.06.043>
- 597 39.Negi M, Chawla PA, Faruk A, Chawla V. Role of heterocyclic compounds in  
598 SARS and SARS CoV-2 pandemic. *Bioorg Chem*. 2020 Nov;104:104315. doi:  
599 10.1016/j.bioorg.2020.104315. Epub 2020 Sep 24. PMID: 33007742; PMCID:  
600 PMC7513919.

- 601 40.Eze FU, Ezeorah CJ, Ogboo BC, Okpareke OC, Rhyman L, Ramasami P,  
602 Okafor SN, Tania G, Atiga S, Ejayi TU, Ugwu MC, Uzoewulu CP, Ayogu JI,  
603 Ekoh OC, Ugwu DI. Structure and Computational Studies of New Sulfonamide  
604 Compound: {(4-nitrophenyl)sulfonyl}tryptophan. *Molecules*. 2022 Oct  
605 31;27(21):7400. doi: 10.3390/molecules27217400. PMID: 36364227; PMCID:  
606 PMC9654880.
- 607 41.Rogosnitzky M, Okediji P, Koman I. Cepharanthine: a review of the antiviral  
608 potential of a Japanese-approved alopecia drug in COVID-19. *Pharmacol Rep*.  
609 Dec 2020;72(6):1509-1516. doi:10.1007/s43440-020-00132-z
- 610 42.Chen YL, Chen CY, Lai KH, Chang YC, Hwang TL. Anti-inflammatory and  
611 antiviral activities of flavone C-glycosides of *Lophatherum gracile* for COVID-  
612 19. *J Funct Foods*. Feb 2023;101:105407. doi:10.1016/j.jff.2023.105407
- 613 43.He C-L, Huang L-Y, Wang K, et al. Identification of bis-benzylisoquinoline  
614 alkaloids as SARS-CoV-2 entry inhibitors from a library of natural products.  
615 *Signal Transduction and Targeted Therapy*. 2021/03/23 2021;6(1):131.  
616 doi:10.1038/s41392-021-00531-5
- 617



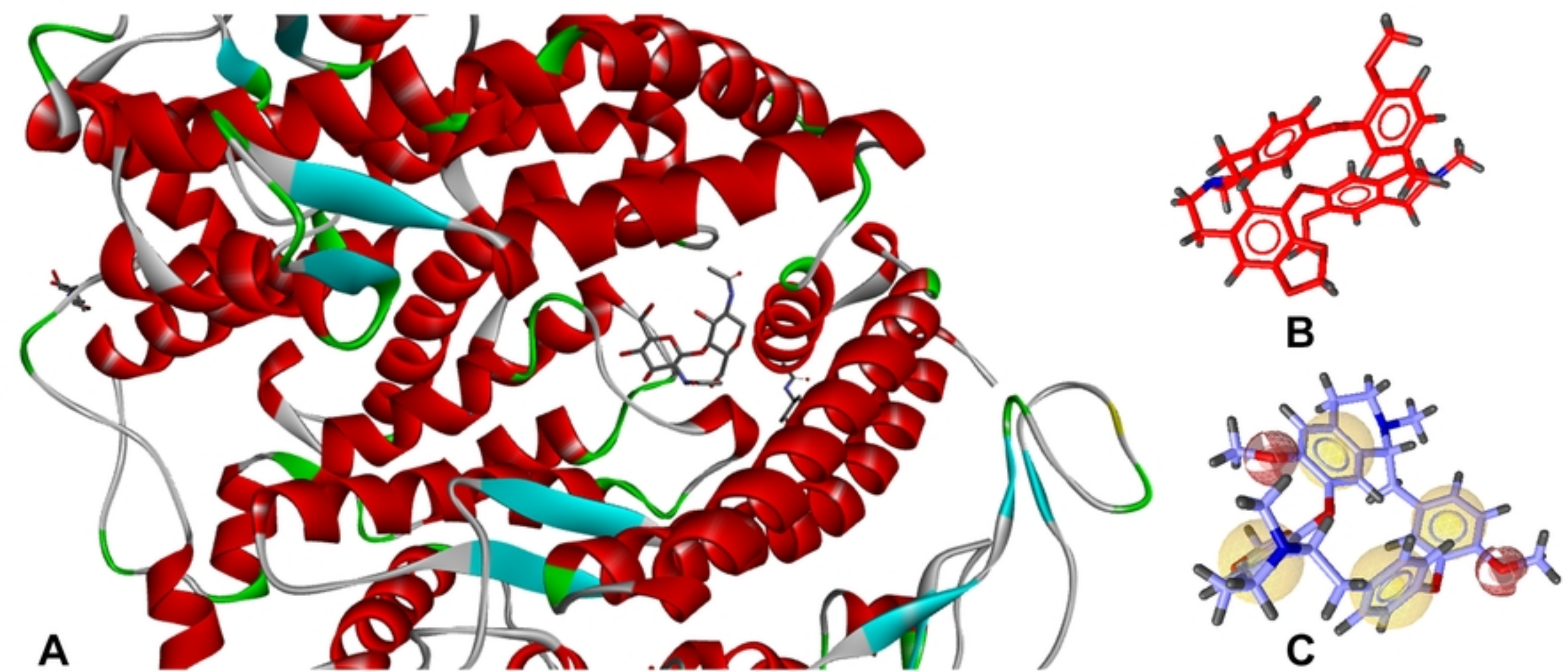
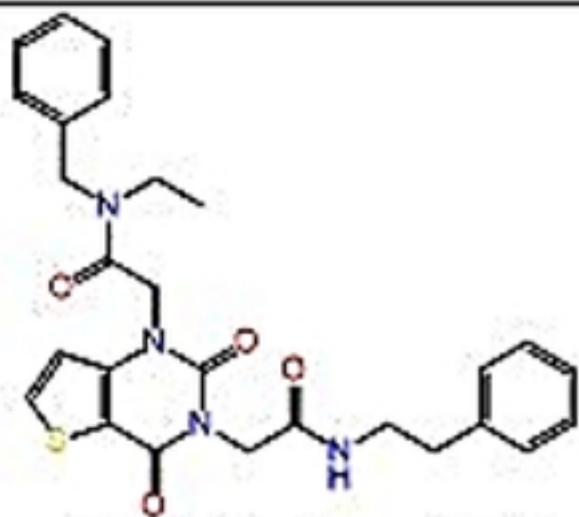


Figure 2

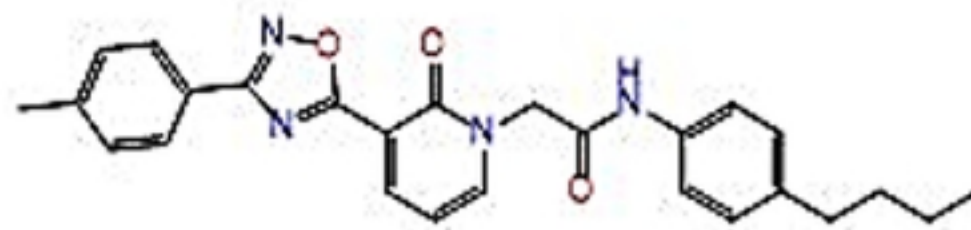
Structure formula/ IUPAC Name



N-benzyl-2-(2,4-dioxo-3-(2-oxo-2-(phenethylamino)ethyl)-3,4-dihydrothieno[3,2-d]pyrimidin-1(2H)-yl)-N-ethylacetamide

**Hit2**

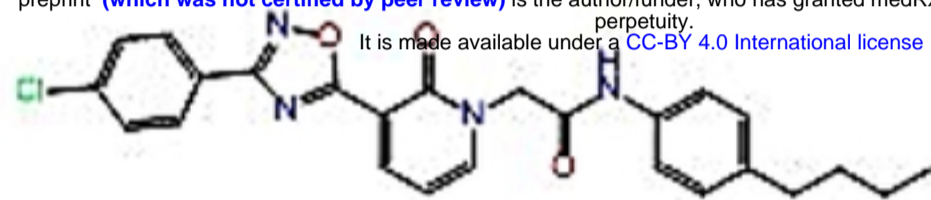
Structure formula/ IUPAC Name



N-(4-butylphenyl)-2-(2-oxo-3-(3-(p-tolyl)-1,2,4-oxadiazol-5-yl)pyridin-1(2H)-yl)acetamide

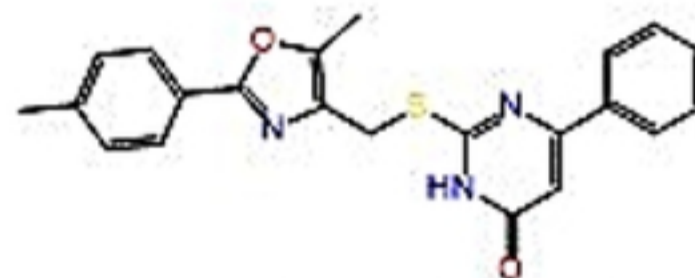
**Hit3**

medRxiv preprint doi: <https://doi.org/10.1101/2024.11.06.24316825>; this version posted November 11, 2024. The copyright holder for this preprint (which was not certified by peer review) is the author/funder, who has granted medRxiv a license to display the preprint in perpetuity. It is made available under a [CC-BY 4.0 International license](https://creativecommons.org/licenses/by/4.0/).



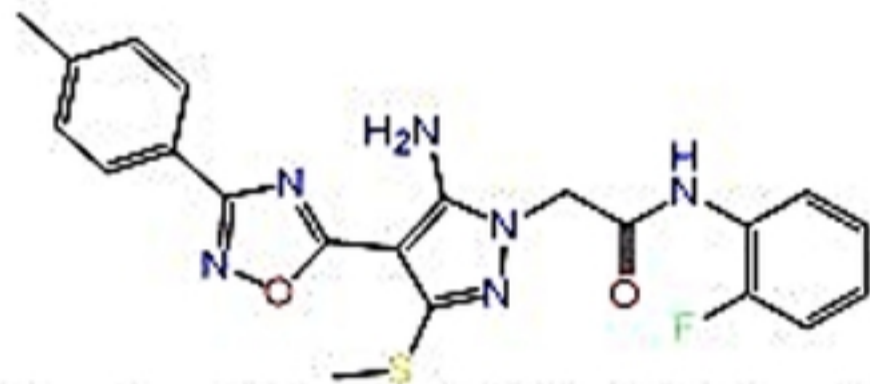
N-(4-butylphenyl)-2-(3-(3-(4-chlorophenyl)-1,2,4-oxadiazol-5-yl)-2-oxopyridin-1(2H)-yl)acetamide

**Hit5**



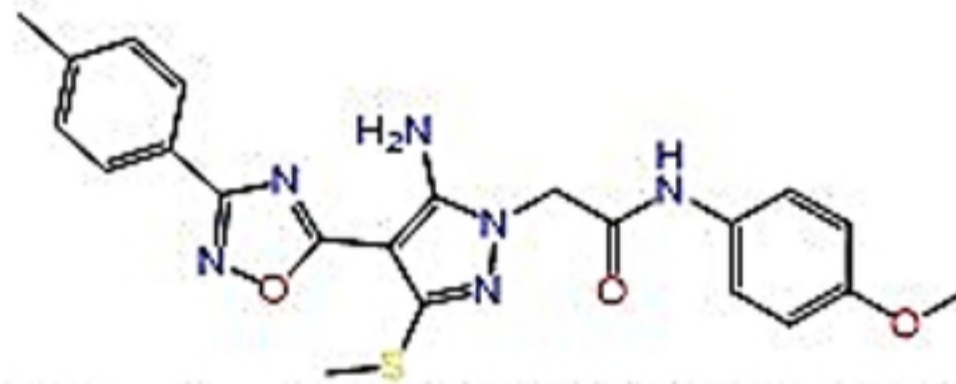
2-(((5-methyl-2-(p-tolyl)oxazol-4-yl)methyl)thio)-6-phenylpyrimidin-4(3H)-one

**Hit7**



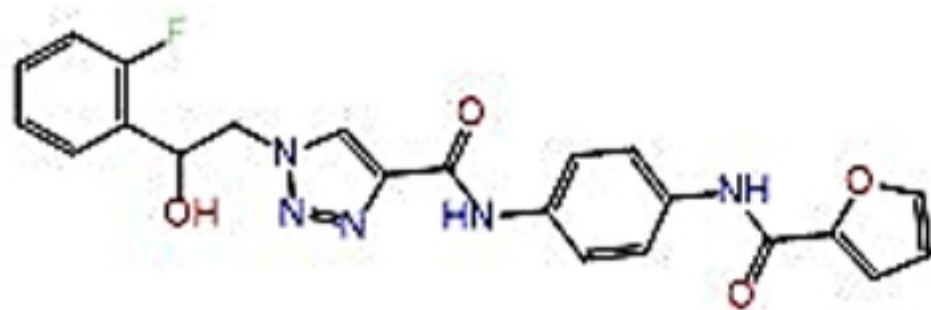
2-(5-amino-3-(methylthio)-4-(3-(p-tolyl)-1,2,4-oxadiazol-5-yl)-1H-pyrazol-1-yl)-N-(2-fluorophenyl)acetamide

**Hit9**



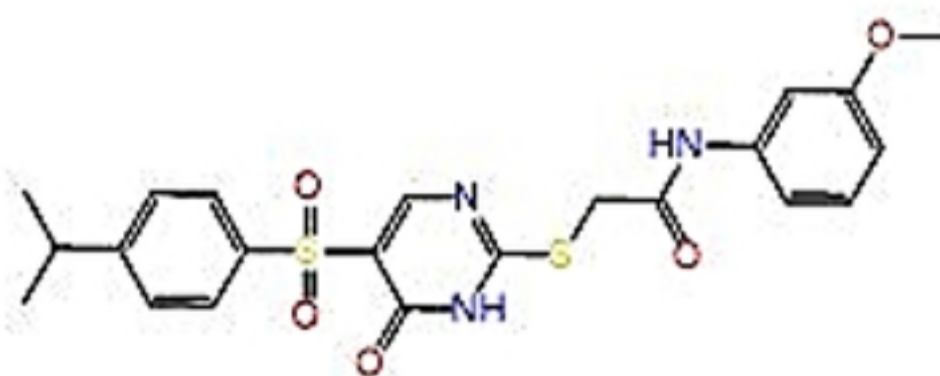
2-(5-amino-3-(methylthio)-4-(3-(p-tolyl)-1,2,4-oxadiazol-5-yl)-1H-pyrazol-1-yl)-N-(4-methoxyphenyl)acetamide

**Hit10**



1-(2-(2-fluorophenyl)-2-hydroxyethyl)-N-(4-(furan-2-carboxamido)phenyl)-1H-1,2,3-triazole-4-carboxamide

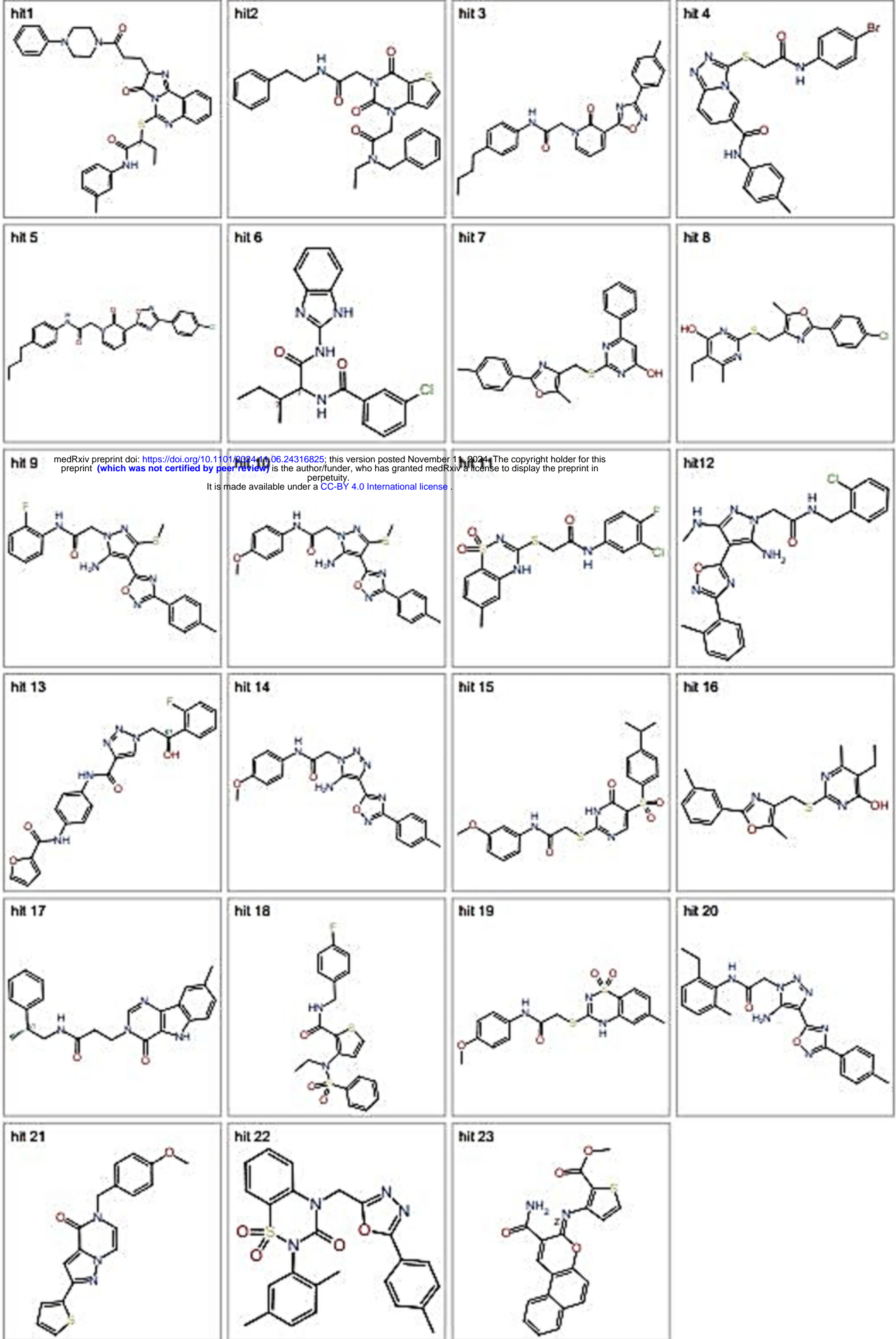
**Hit13**



2-(((5-((4-isopropylphenyl)sulfonyl)-6-oxo-1,6-dihydropyrimidin-2-yl)thio)-N-(3-methoxyphenyl)acetamide

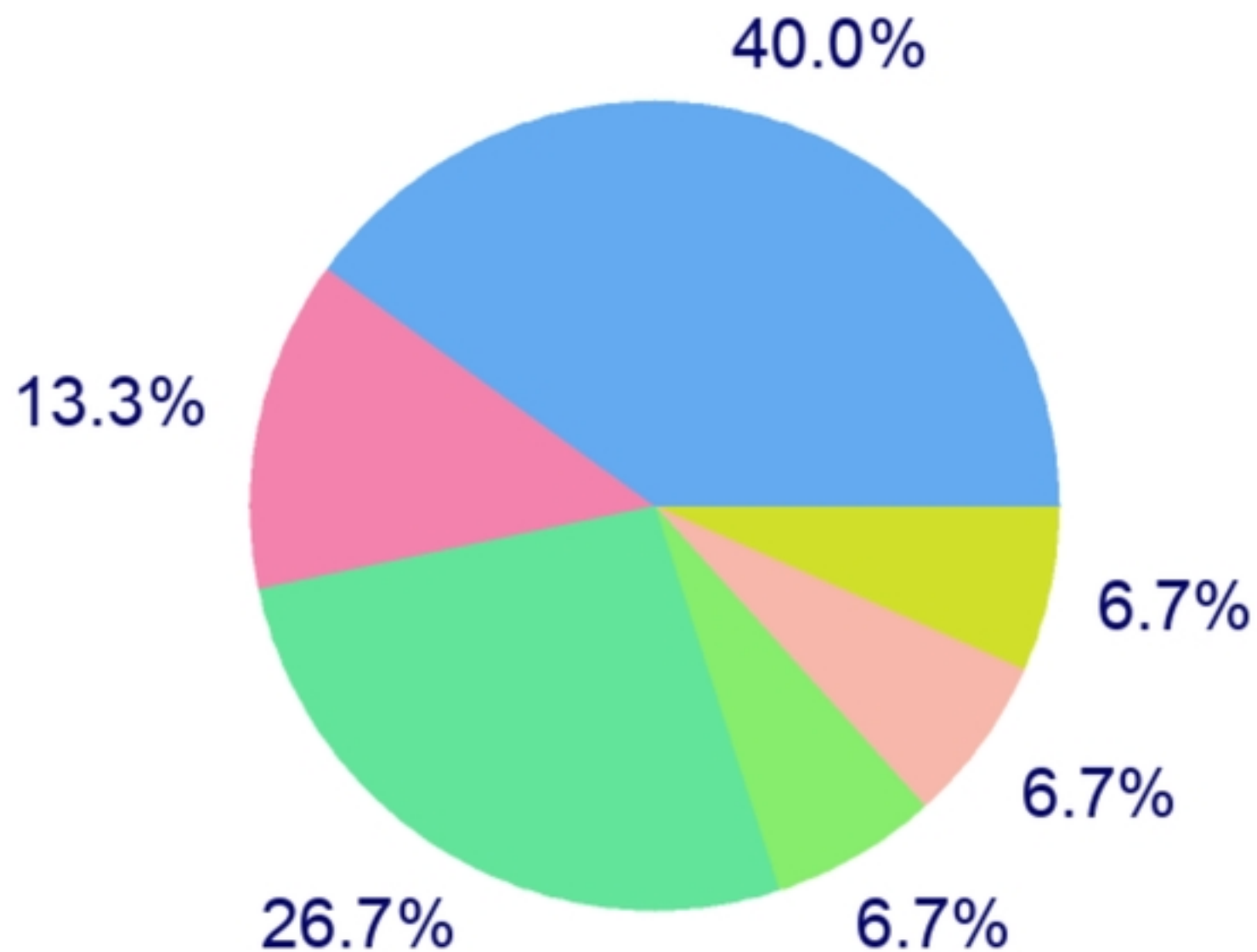
**Hit15**

Figure 1



medRxiv preprint doi: <https://doi.org/10.1101/2024.11.06.24316825>; this version posted November 11, 2024. The copyright holder for this preprint (which was not certified by peer review) is the author/funder, who has granted medRxiv a license to display the preprint in perpetuity. It is made available under a [CC-BY 4.0 International license](https://creativecommons.org/licenses/by/4.0/).

Figure 3



- Family A G protein-coupled receptor
- Electrochemical transporter
- Ligand-gated ion channel
- Hydrolase
- Phosphodiesterase
- Surface antigen

Figure 4

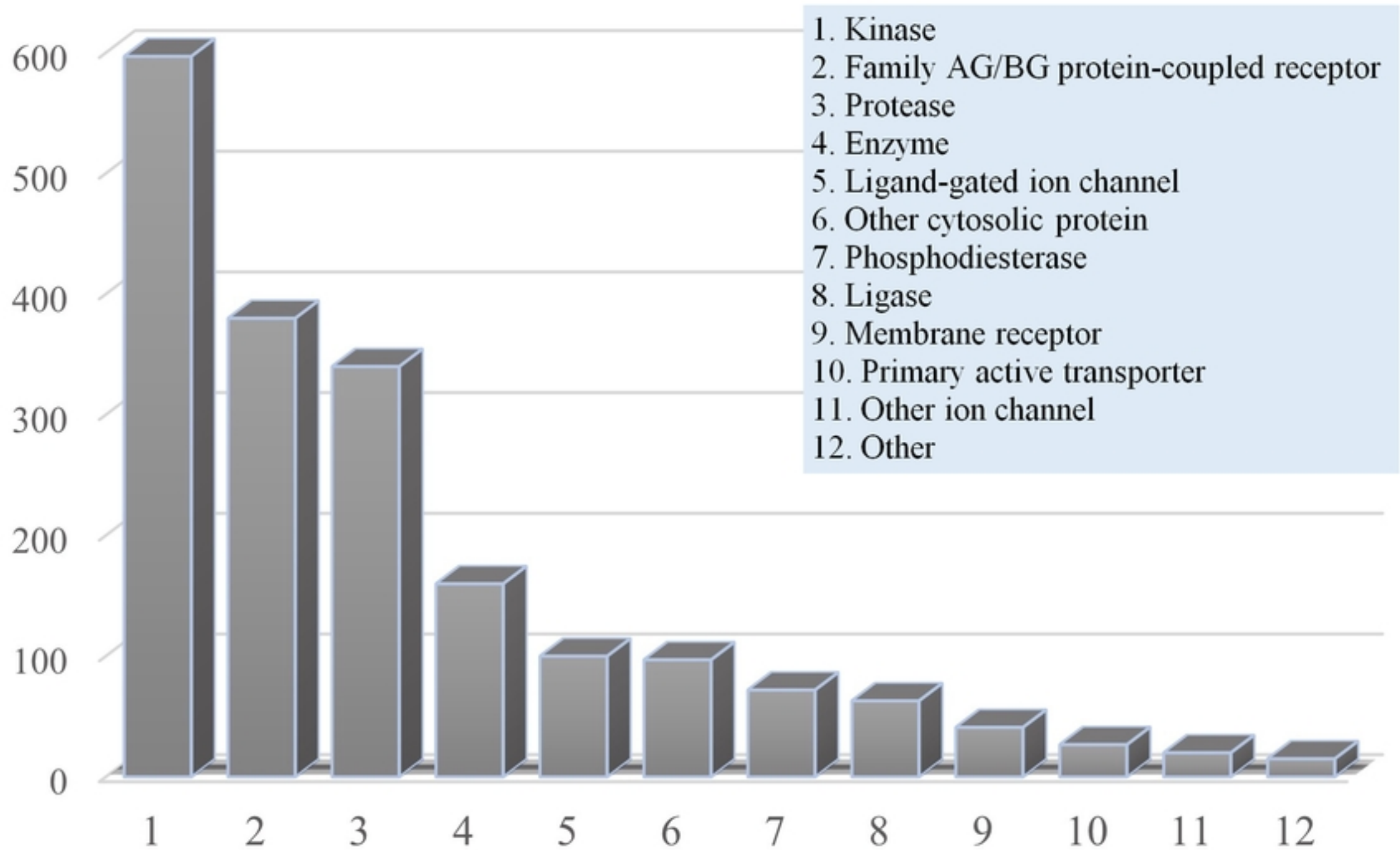
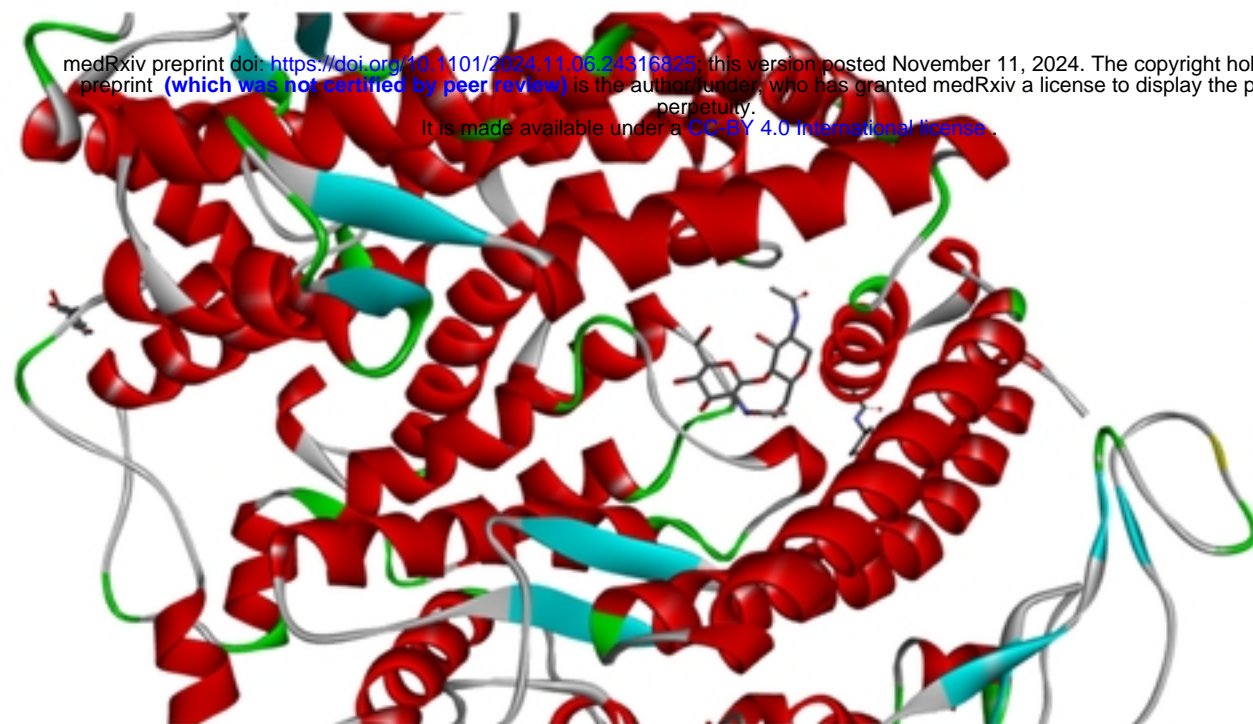
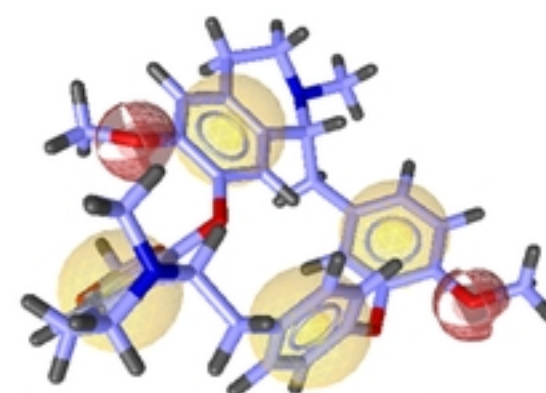


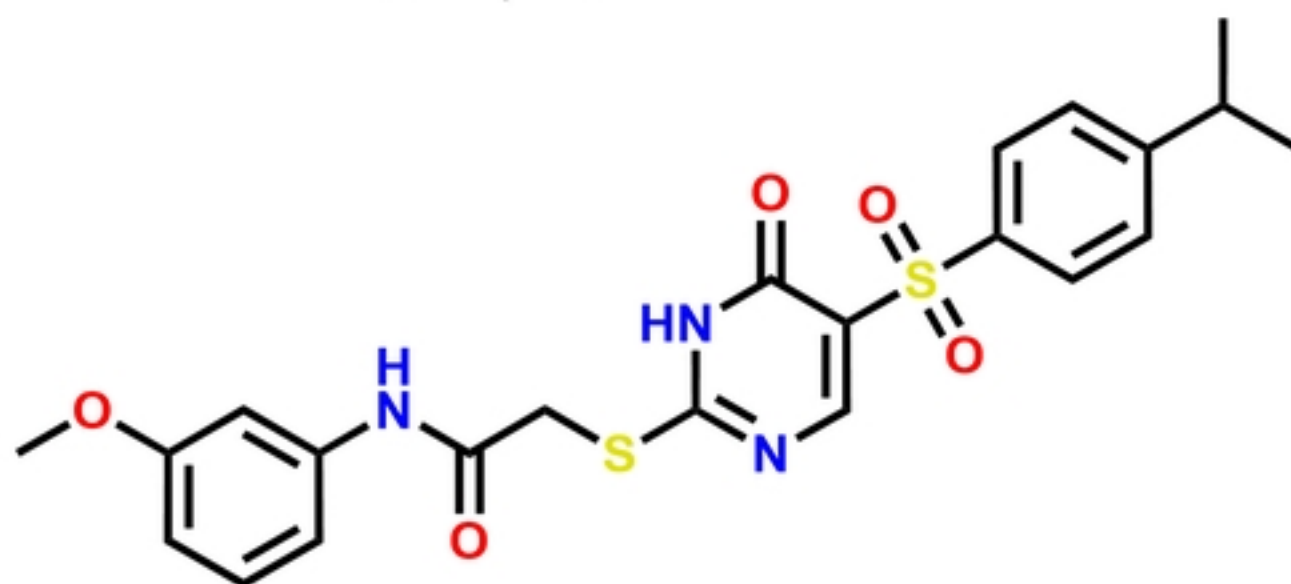
Figure 5



**ACE2, PDB: 7WBP**



**CEP**



**IN VITRO**

**DOCKING PDB:  
4E4L, 4D1S, 4Z16,  
1ALU, 7WOF, 7LLZ**

**DOCKING  
ACE2**

